Journal of Sustainable Development of Smart Energy Networks

http://www.sdewes.org/jsdsen

Year 2026, Volume 1, Issue 1, 2030685

Original Research Article

Experimental and Numerical Investigation of PCM-Based Cold Thermal Energy Storage for Power-to-Thermal Integration in 4GDHC Networks

Francesco Liberato Cappiello[1], Luca Cimmino[2*], Maria Vicidomini[3], Guido Liguori[4]
Department of Industrial Engineering, University of Naples Federico II,
P.le Vincenzo Tecchio, 80, 80125, Napoli, NA
e-mail: francescoliberato.cappiello@unina.it, luca.cimmino@unina.it, maria.vicidomini@unina.it, guido.liguori@studenti.unina.it

Cite as: Cappiello, F. L., Cimmino, L., Vicidomini, M., Liguori, G. Experimental and Numerical Investigation of PCM-Based Cold Thermal Energy Storage for Power-to-Thermal Integration in 4GDHC Networks, J. sustain. dev. smart. en. net., 1(1), 2030685, 2026, DOI: https://doi.org/10.13044/j.sdsen.d3.0685

ABSTRACT

This work focuses on Cold Thermal Energy Storage (CTES), a technology that has attracted growing interest in recent years and represents a key element for achieving the European decarbonisation targets. Among the available technologies, Phase Change Materials (PCMs) represent a promising solution due to their high energy density; however, their widespread adoption remains limited by slow solidification kinetics and the formation of an insulating solid layer around the heat exchanger, which significantly increases the charging time. This work addresses these limitations through a combined experimental and numerical investigation on SP9 GEL, a low-temperature PCM supplied by Rubitherm. A five-month laboratory campaign was carried out at the Process and Energy Laboratory of Delft University of Technology to identify an effective and rapid solidification strategy. Based on the experimental outcomes, the PCM was integrated into the existing 4th-generation district heating and cooling (4GDHC) network of the "Grande Sud" shopping mall in Naples, Italy. A dynamic simulation in TRNSYS 18 was performed to evaluate the performance of CTES under realistic operating conditions during a representative summer day. Despite the partial stratification caused by the large tank height, the PCM tank allowed the complete shutdown of the heat pumps for approximately four hours in the afternoon. On the same day, 72.39% of the photovoltaic surplus was stored as thermal energy instead of being exported to the grid, confirming the effectiveness of the Power-to-Thermal (P2T) strategy under high solar availability. These findings show that cold thermal storage can serve as an effective reservoir for surplus electricity generated by non-dispatchable renewable energy sources. However, realising this potential requires careful consideration of the operating conditions, the selection of a PCM suited to the target application, and a tank design capable of exploiting the entire available storage volume.

KEYWORDS

Cold Thermal Energy Storage (CTES), Phase Change Material (PCM), Experimental analysis, Renewable energy, Dynamic simulation, Energy management strategy.

INTRODUCTION

Energy stands at the heart of modern civilization, influencing economic, social, and environmental dynamics worldwide. Yet the current paradigm, still heavily dependent on centralized and fossil-based energy systems, is increasingly incompatible with both climate goals and the pursuit of universal access to clean resources. In this context, the ongoing energy transition requires a shift toward decentralized, resilient configurations in which renewable sources, energy efficiency, and storage technologies play a central role.

Heating and cooling are among the main contributors to global energy consumption and greenhouse gas emissions. Alongside transportation, these fields represent a substantial share of final energy use, with thermal comfort in buildings alone representing nearly 30% of global final demand and over 25% of energy-related CO_2 emissions [1]. While heating has traditionally dominated this share, rising global temperatures and improved living standards are rapidly increasing the demand for cooling, especially in urban environments, making sustainable cooling a major challenge for the coming decades.

District Heating and Cooling (DHC) networks are increasingly recognized as strategic infrastructures in the sustainable transformation of urban energy systems. By harnessing renewable sources and recovering waste heat from industrial processes, they offer a scalable and adaptable approach to decarbonizing thermal energy use across multiple sectors. Among the different generations of DHC systems, fourth-generation district heating and cooling (4GDHC) systems distinguish themselves through smart control, low-temperature operation, and high levels of sector integration, making them especially suited to the development of climate-neutral cities.

To fully unlock the potential of these networks, thermal energy storage (TES) plays a crucial role by decoupling energy supply from demand in time. Among the various TES technologies, Phase Change Materials (PCMs) have gained particular attention for their ability to store and release large amounts of energy within narrow temperature ranges. When applied to cooling systems, CTES can be charged during night-time hours, when electricity is cheaper and the grid is less stressed, and discharged during the day to meet peak cooling loads. This strategy, known as peak shaving and load shifting, enhances grid stability, optimizes energy use, and reduces operational costs. Moreover, thermal storage enables Power-to-Thermal strategy, where excess renewable electricity, often produced at times of low demand, is converted into thermal energy, stored, and later used when needed. This improves self-consumption, strengthens user autonomy, and minimizes electricity injections into the grid.

The growing interest in PCM-based storage has led to several experimental and real-world implementations. A notable example is the 2014 installation at Bergen University in Norway, where a salt hydrate PCM was used in combination with a 1.4 MW chiller to cover a peak cooling load of 3 MW. The system consisted of four 60 m³ tanks, each filled with FlatICE containers, reaching a total storage capacity of 11,200 kWh. Charged at night and discharged during the day, the setup also included 81 geothermal boreholes for seasonal storage. However, as shown in the performance assessment by Jokiel [2], the system operated below its potential due to subcooling effects and uneven heat transfer caused by natural convection, especially during the melting phase.

A second case is the installation at an educational facility in Melbourne, Australia, where 5,120 FlatICE panels containing PCM were arranged in 40 m³ of insulated tanks to support the building's cooling system. Charging relied on nighttime temperatures falling below 11 °C, with water used as the heat transfer medium. Alam *et al.* [3] observed that only 15% of the theoretical storage capacity was effectively utilized, mainly due to insufficient night-time cooling during summer and the high electricity consumption of auxiliary equipment, revealing a considerable mismatch between design expectations and real-world performance.

A further study by Tan *et al.* [4] focused on a district cooling application in Gothenburg, Sweden, where Rubitherm SP11, chemically similar to the SP9 GEL analyzed in this study, was used in a PCM storage tank integrated with a district loop. Despite an initial design capacity of 275 kWh, the actual system underperformed due to limited charge/discharge rates and the parasitic consumption of auxiliary components. Additionally, the economic evaluation revealed that high capital costs and operational inefficiencies hindered financial viability.

These case studies clearly illustrate both the potential and the limitations of PCM-based TES in real settings. While promising in concept, the translation of lab-scale performance into fully operational, efficient storage systems remains a significant challenge. In particular, few

studies have addressed the behaviour of low-temperature PCMs within dynamically operated 4GDHC networks, highlighting a critical research gap in terms of experimental validation and system-level integration.

This study seeks to bridge that gap by combining laboratory-scale characterization of a commercial salt hydrate PCM, with a detailed performance assessment through dynamic simulation in TRNSYS. The experimental activity is used to characterize the material's charging and discharging dynamics, effective phase change temperature range, and thermal response under operating conditions relevant for low-temperature cooling storage. These results are then employed to calibrate the PCM storage component within an already validated TRNSYS model, enabling a consistent evaluation of the material's behaviour at system scale.

By linking experimentally derived PCM properties to the operational dynamics of a real 4GDHC network, this work offers new insights into the practical feasibility of PCM-based cold thermal storage as a key enabler for future low-carbon and renewable-integrated urban infrastructures.

MATERIALS AND METHODS

This section outlines the materials, instrumentation and experimental procedures used to investigate the thermal response of the selected PCM under controlled laboratory conditions.

The configuration of the setup, the measurement strategy and the operating conditions adopted during the charging and discharging cycles are presented in a systematic manner.

The aim is to propose a solution that reduces the charging time, a critical limitation that may otherwise prevent the use of low-temperature thermal storage in industrial applications.

Phase Change Material - SP9 GEL

SP9 GEL is an inorganic phase change material from the SP product series manufactured by Rubitherm GmbH. It is a salt hydrate-based compound composed of a mixture of salt, water and specific additives designed to enhance thermal and physical stability.

This PCM is widely used in both active and passive heating and cooling systems, including air-conditioning units and integrated roof and wall elements, due to its efficient thermal energy storage and release capabilities. Main properties adopted in the present analysis, all derived from the manufacturer's datasheet, are reported in **Table 1**.

Table 1. SP9 GEL properties

Parameter	Value
Melting area	10 °C – 11 °C
Congealing area	7 °C – 9 °C
Phase change enthalpy	136 $\frac{kJ}{kg}$
Heat conductivity	0.6 $\frac{W}{m\,K}$
Density solid	1.4 $\frac{kg}{L}$
Density liquid	1.3 $\frac{kg}{L}$

A key advantage of the material lies in its stable performance over repeated phase change cycles, ensuring consistent thermal behaviour during long-term operation. It also demonstrates limited supercooling, typically ranging from 2 to 3 K depending on the volume and cooling rate, which helps maintain predictable melting and solidification processes. Furthermore, its low flammability and non-toxic composition make it a safe and reliable option for thermal energy storage applications

Experimental Setup

To evaluate the performance of a phase change material potentially suitable for integration with Heating, Ventilation, and Air Conditioning (HVAC) systems, an experimental campaign was carried out at the Process & Energy laboratory of Delft University of Technology.

The experimental setup (**Figure 1** and **Figure 2**) was designed to be simple yet effective, enabling precise thermal assessment during the phase change process. It consisted of the following main components: a cooling thermostat for system temperature control, a dedicated PCM enclosure where the material was housed and monitored, and several thermocouples connected to a Data Acquisition system (DAQ), which continuously recorded temperature data in real time. A flow meter was used to measure the circulation rate of the cooling fluid, while expanded polystyrene (EPS) panels were employed to provide thermal insulation. A GoPro camera was used for visual monitoring and time-lapse recording, with an LED strip installed to illuminate the enclosure and enhance the visual clarity of the phase change process during video recordings.

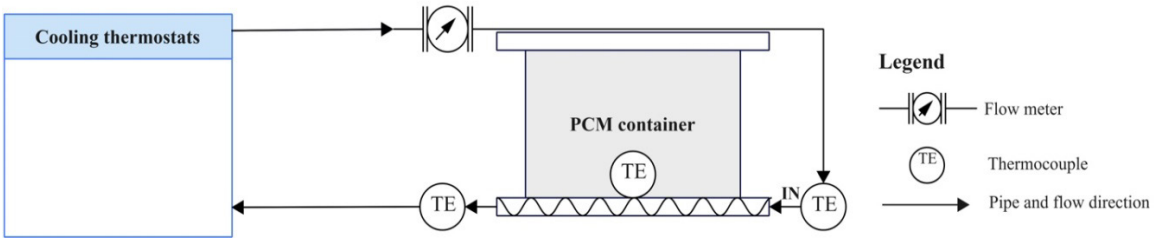

Figure 1. Schematic representation of the experimental setup

The experimental investigation aimed to characterize the thermal behavior of the selected PCM under controlled cooling and heating conditions. Specifically, the following objectives were established:

- To determine the duration of both charging and discharging processes;
- To monitor the temperature evolution of the PCM, highlighting key features such as the melting and solidification plateaus;
- To evaluate different charging methods.

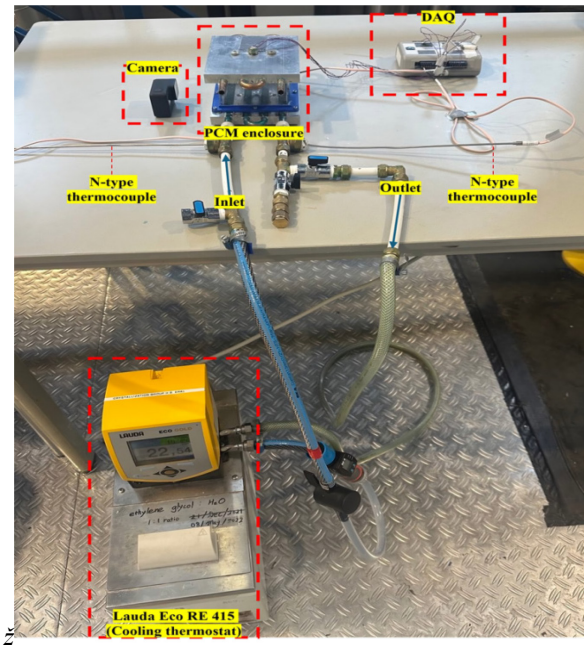

Figure 2. Experimental setup

Cooling thermostat. The thermal control of the experimental system was ensured by a Lauda Eco RE 415 thermostat (**Figure 3**), a versatile unit capable of both heating and cooling the working fluid. Equipped with an integrated circulation pump, the device provides a steady flow through the circuit, enabling efficient heat exchange with the PCM enclosure during both charging and discharging phases.

The unit is equipped with a 4L thermostatic bath and a digital display for setting the desired set point, which is then accurately maintained through automated control. The system offers high thermal stability, with temperature fluctuations limited to ±0.02 K, making it ideal for experiments that require consistent and accurate control of thermal conditions.

Figure 3. Lauda Eco RE 415

Enclosure

The Phase Change Material was placed inside a custom-designed plexiglass container with internal dimensions of 100 mm × 100 mm × 50 mm and a wall thickness of 4 mm (**Figure 4**).

Thermal exchange between the PCM and the working fluid was enabled using two tubed cold plates from Wakefield Thermal. The lower plate served as the main interface for heat transfer, while the upper one functioned as a lid, effectively sealing the system.

Inside the container, five T-type thermocouples were installed at 1 cm intervals and mounted on a PETG 3D-printed support placed at the centre of the enclosure.

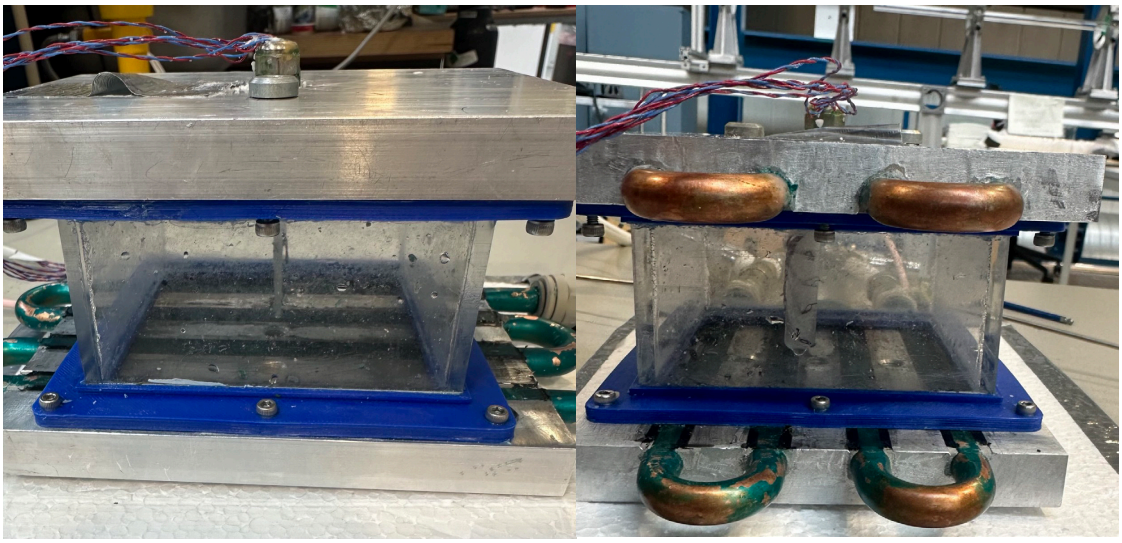

Figure 4. PCM enclosure: frontal view (a); lateral view (b)

To minimise heat losses and ensure better thermal isolation from the surrounding environment, the container was enclosed within a set of expanded polystyrene panels. As a consequence of this opaque configuration, a quantitative determination of phase fractions during solidification was not possible. Future work could address this limitation through the use of transparent enclosures or enthalpy-based measurement approaches.

The properties of the insulating material are detailed in **Table 2**, which summarises thermal conductivity and resistance, along with operational temperature range suitable for the scope of the experimental campaign:

Table 2. EPS material properties

Parameter	Value
Thickness	20 mm
Operating temperature range	-40 °C to +70 °C
λ	0.03 $\frac{\mathrm{W}}{\mathrm{m\,K}}$
R_d	0.50 $\frac{\mathrm{m^2\,K}}{\mathrm{W}}$

Figure 5. EPS panels

Thermocouples

Seven thermocouples were used to monitor the system temperature: five type T sensors were placed inside the PCM container, while two type N probes were installed at the inlet and outlet of the heat exchanger.

To ensure the reliability of the measurements, an uncertainty evaluation was performed. The first step consists in defining the absolute error, expressed as the difference between the measured value X_m, and the true value, X_t. This term quantifies the systematic deviation of the thermocouple from the reference value and is calculated as:

$$u_\mathrm{abs} = |X_\mathrm{m} - X_\mathrm{t}| \tag{1}$$

The calibration was carried out using ice as the reference medium, assuming a true temperature of 0 °C. The deviation of each thermocouple from this reference provided the systematic component of the uncertainty.

The random component was evaluated as a Type A contribution following the Guide to the Expression of Uncertainty in Measurement (GUM) [5]. For each thermocouple, 100 measurements (N) were collected under repeatable conditions, and the standard deviation (s) of these readings was used to compute the random uncertainty:

$$u_{\mathrm{r}} = \frac{s}{\sqrt{N}} \tag{2}$$

Finally, the absolute error and the random uncertainty were combined using the Root Sum Square (RSS) method to obtain the total uncertainty of the thermocouples according to:

$$u = \sqrt{u_{\mathrm{abs}}^2 + u_{\mathrm{r}}^2} \tag{3}$$

The results of this calibration procedure, detailing the uncertainties associated with each thermocouple, are presented in Table 3.

Table 3. Thermocouple types and measurement uncertainties

Probe	Type	Uncertainty
Thermocouple 1	T	± 0.46 °C
Thermocouple 2	T	± 0.68 °C
Thermocouple 3	T	±0.81 °C
Thermocouple 4	T	± 0.65 °C
Thermocouple 5	T	± 0.90 °C
Thermocouple 6	N	± 0.11 °C
Thermocouple 7	N	± 0.10 °C

Data Acquisition System

To enable real-time data visualisation and streamline subsequent analysis, all thermocouples were connected to an OM-DAQ-USB-240 data acquisition system. The module provided stable, high-resolution conversion of voltage signals into temperature data, while the DAQ Central software offered intuitive configuration, continuous monitoring of the readings and automatic export of the recorded profiles for post-processing.

Discharging Procedure

At the starting point, the phase change material was in a fully solid state. The subsequent step consisted of the discharging process, here defined as the transition from solid to liquid, during which the PCM absorbs thermal energy.

The operating conditions were kept consistent with those later adopted in the charging stage, with the sole difference that the ethylene glycol – water mixture supplied by the thermostat was set to a temperature of 17 °C.

During both charging and discharging phases, the temperature of the heat transfer fluid was set to ensure a constant temperature difference of 6.5 °C relative to the main phase change peak of the PCM. This condition provided a sufficient thermal driving force for heat exchange, promoting the completion of the phase transition within controlled and reproducible operating conditions.

Charging Procedure

Once the discharging stage was completed and the PCM was brought to a liquid state, the charging phase was initiated. The cooling thermostat supplied a constant flow rate of 3.1 L/min of ethylene glycol-water solution, maintained at a temperature of 2 °C.

EXPERIMENTAL RESULTS

One of the main objectives of the experimental campaign was to evaluate the time required to charge the phase change material using different operating strategies. In this context, the charging time is defined as the duration necessary for the entire PCM volume to reach a temperature equal to or lower than the peak point of the congealing area, identified at 8.5 °C.

Three different methods were tested to assess their effectiveness in reducing the recharge duration. Temperature readings were recorded every second at three key locations: within the PCM, at the inlet, and at the outlet of the embedded serpentine coil.

Method 1

In the first configuration, a total mass of 0.45 kg of SP9 GEL was cooled exclusively from the bottom.

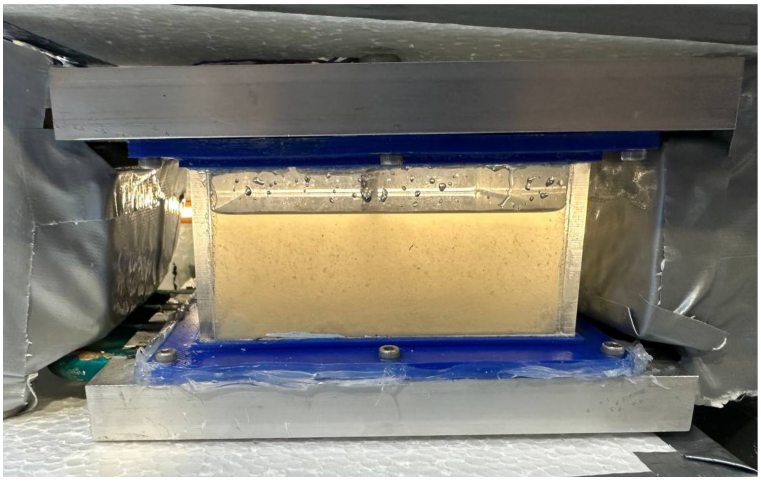

Figure 6. PCM at t = 0

Prior to the charging process, a pre-cooling step was performed to bring the material to an initial temperature of approximately 20 °C. The heat transfer fluid was maintained at 2 °C, and under these conditions the measured recharge time for the system was 4.75 hours (**Figure 7**).

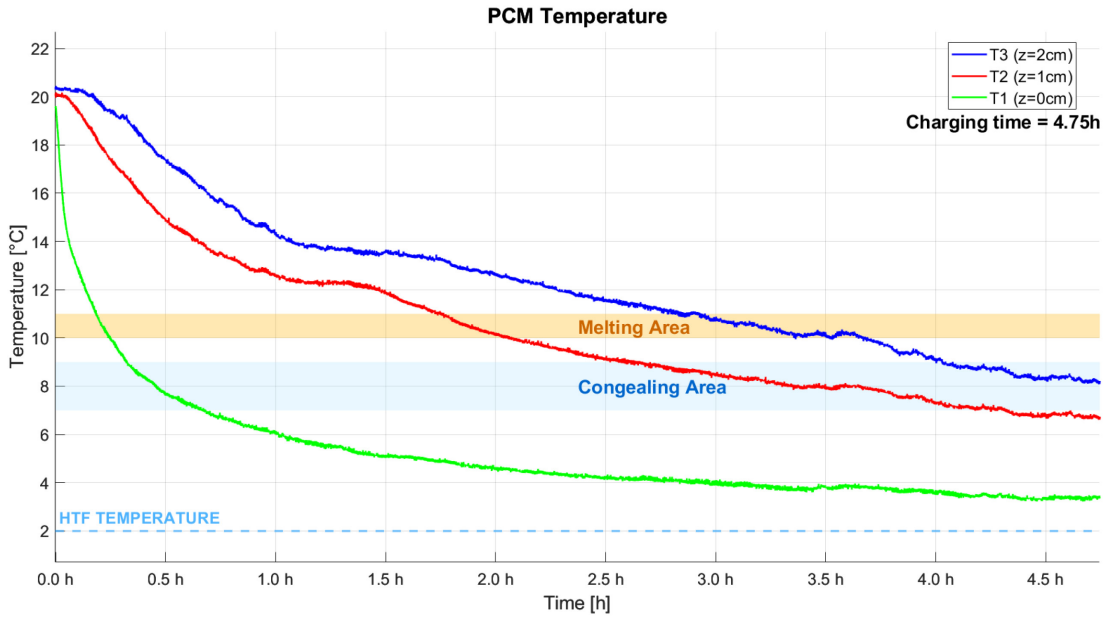

Figure 7. Results with the first method: PCM temperature over time during charging

The temperature profiles reveal a marked vertical stratification from the onset of the charging phase, leading to a small temperature difference between the inlet and outlet of the serpentine coil and consequently, limited heat-exchange efficiency.

During the early stage, heat transfer was driven by natural convection and conduction, leading to relatively fast solidification near the coil. This behaviour is confirmed by thermocouple T1, located close to the heat exchanger, which reached the solidification peak within the first 30 minutes (**Figure 8**), indicating the rapid formation of a solid layer around the coil.

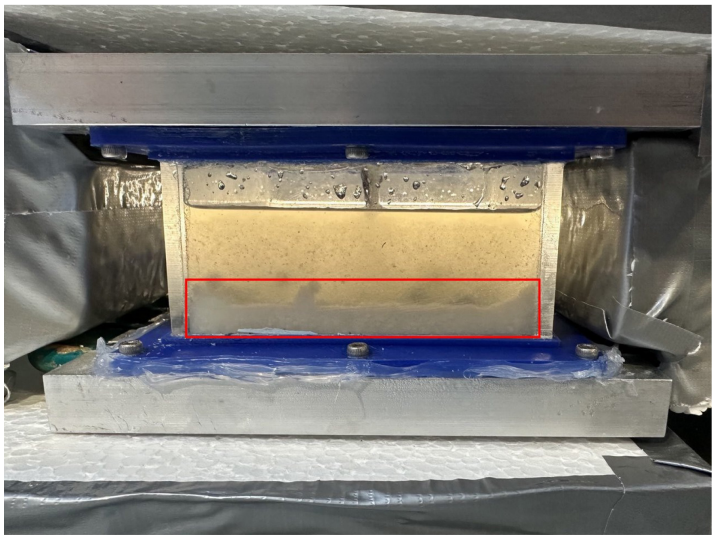

Figure 8. PCM at t = 30 min, with solid layer highlighted in red

Once this layer formed, convective heat transfer was progressively suppressed, and conduction became the dominant mechanism. This outcome reflects a well-known limitation of PCMs: as the solid region thickens, natural convection is inhibited, and conduction alone, limited by the low thermal conductivity of the material, is insufficient to sustain a fast or uniform solidification. In industrial applications, this issue is commonly addressed by installing additional heat exchangers in the upper and central sections of the enclosure to enhance thermal penetration throughout the entire PCM volume.

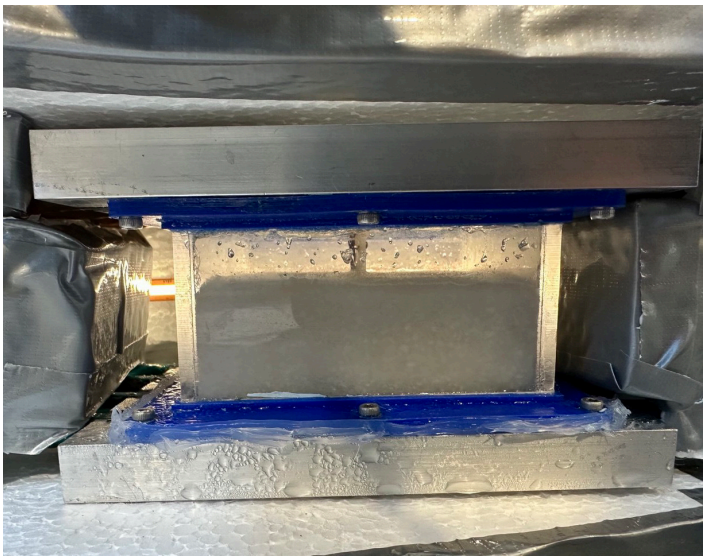

Figure 9. PCM at t = 4.75 h

In contrast, during the discharging phase the density difference between solid and liquid phases enhanced upward convection of the lighter liquid fraction.

This mechanism favoured a more uniform temperature distribution within the PCM and led to a complete discharging time of 1.52 hours, which explains why the experimental campaign primarily focused on the charging process.

Method 2

With the aim of reducing the time required for PCM solidification, an alternative configuration was designed to increase the effective heat exchange surface. A mass of 0.225 kg of SP9 GEL, corresponding to half the quantity used in Method 1, was distributed into eight syringes (**Figure 10**), thereby shifting from a rectangular geometry to a cylindrical one.

Figure 10. PCM inside syringes

The enclosure was then filled with water, with the syringes were fully immersed. In this configuration, maintaining the heat transfer fluid (HTF) temperature at 2 °C prevented the water from freezing, ensuring that heat exchange was not limited to conduction, as in the previous configuration.

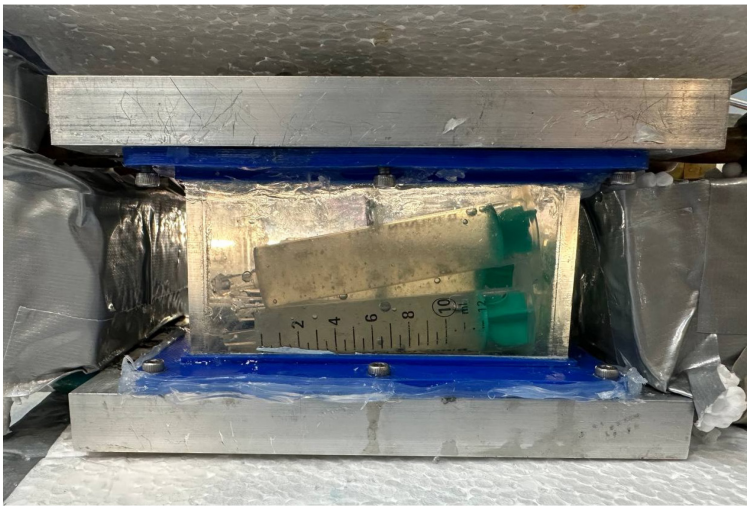

Figure 11. Charging with the 2° method

Nevertheless, the results were not particularly encouraging. A complete solidification of the PCM required approximately 3 hours (**Figure 12**). Although this might seem like an improvement compared to Method 1, it must be emphasized that the amount of material processed was only half of that in the previous test.

Figure 12. PCM at t = 3 h

Several factors contributed to this slower charging rate. First, the syringes were made of plastic, a material characterized by low thermal conductivity, which significantly limited the efficiency of heat transfer between the water and the PCM. Furthermore, since the entire enclosure was filled with water, cooling the upper section of the volume demanded additional time, as the system still relied primarily on bottom cooling.

Method 3

Given the limitations observed in the previous methods, a third strategy was tested, involving rotation of the PCM enclosure every 30 minutes. The rationale behind this approach was to promote mixing within the material, reduce temperature stratification, and potentially shorten the overall charging time.

A total of 0.45 kg of SP9 GEL was placed inside the container. Two additional pipes were also integrated into the setup, enabling the use of the upper heat exchanger once the system was rotated. The procedure aimed to create a first solid layer during the initial 30 minutes of operation. Once this layer was formed, the corresponding valves were closed to interrupt the refrigerant flow in that section, ensuring a stable temperature. The container was then rotated so that the remaining liquid fraction of the PCM, initially located in the upper part, moved downward and came into direct contact with the refrigerant through the second heat exchanger.

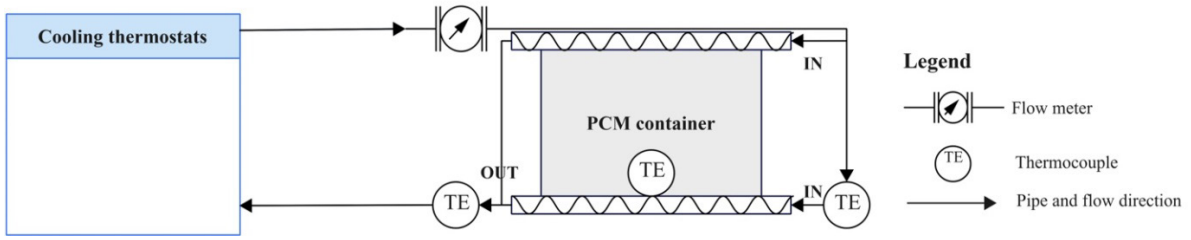

Figure 13. Modified experimental setup

This configuration produced excellent results. The solidified fraction adhered to the exchanger surface, while the rotation allowed the entire liquid portion to relocate to the bottom, where active heat exchange occurred. In this way, the portion already solidified was effectively "stored" in a zone no longer directly involved in the cooling process, thus removing the barrier to heat transfer that characterized Method 1 and concentrating thermal exchange on the remaining liquid PCM. As a result, the recharge time was reduced by 72% compared to Method 1, reaching a total of 1.33 hours.

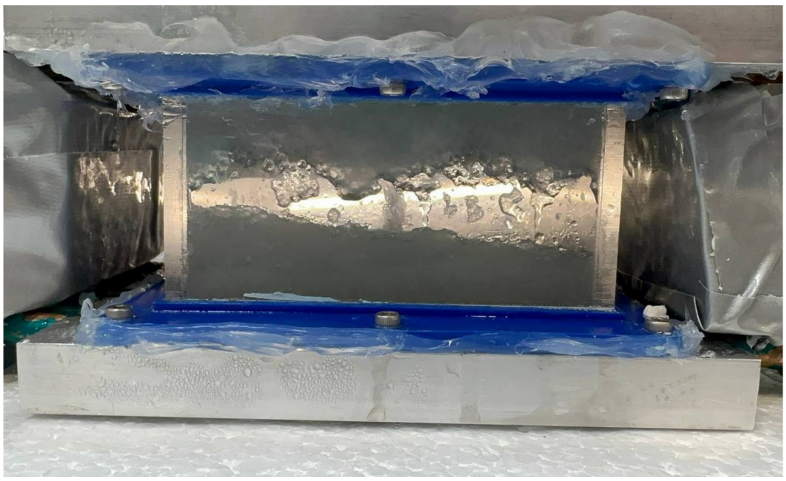

Figure 14. Results obtained with the third method

Discussion and Future Improvements

The comparative evaluation of the three charging strategies highlights how strongly the solidification dynamics of PCMs depend on both heat transfer mechanisms and system geometry.

Method 1 confirmed the intrinsic limitations of using just one heat exchanger, with the rapid formation of a solid layer suppressing convection and leaving conduction as the only active mechanism, thus leading to long charging times.

Method 2, based on the use of syringes, was initially conceived to increase the heat exchange surface. However, the poor thermal conductivity of plastic, combined with the full immersion in water, resulted in the lowest overall performance among the tested strategies. Despite the reduced mass of PCM, solidification was not significantly accelerated, and the approach proved inefficient compared to the other methods.

In contrast, Method 3 clearly demonstrated the benefits of a dynamic configuration. The periodic rotation of the container prevented the solidified fraction from obstructing heat transfer and ensured continuous exposure of the liquid PCM to the refrigerant.

From an industrial perspective, container rotation may not be practical at larger scales; however, several alternative solutions have been proposed in the literature. For example, Zipf *et al.* [6] designed a double-helix structure aimed at reducing the thickness of the solid PCM on the heat transfer surface, thereby improving the overall heat transfer rate.

Other studies have investigated active stirring approaches. Zhang *et al.* [7] developed an anchor-type mechanical stirrer, specifically selected for its ability to overcome the frictional resistance of solidifying paraffin and maintain effective forced convection near the heat transfer surface. This design also operated efficiently at low rotational speeds (10–50 r/min), which are compatible with the timescale of PCM solidification. As a result, the anchor stirrer reduced the total solidification time of paraffin by 48.61% compared to a case without mechanical agitation, demonstrating the significant potential of active stirring systems for enhancing heat transfer in PCM applications.

In addition, enhancement techniques based on modified heat-exchanger geometries have also proven effective. In particular, the application of fins in triplex-tube thermal storage systems increases the effective heat transfer surface area, thereby enhancing conductive heat transfer within the PCM. Such configurations have been shown to improve solidification performance in a simple and cost-effective manner, making fin-based designs an attractive solution for improving heat transfer during phase change without introducing mechanical complexity [8].

Further solutions could also be explored. Among them, laser-induced crystallization employs a localized beam to initiate nucleation at specific points within the PCM, fostering solid formation in multiple regions and potentially reducing stratification while improving uniformity during solidification. Another possibility is finger cooling, in which several slender cooling elements are distributed throughout the PCM volume. By extracting heat at multiple locations, this configuration increases the effective exchange surface and shortens the conductive path, which may accelerate the overall charging process.

CASE STUDY

To better understand the potential of CTES, this section explores the integration of the SP9 GEL within a fourth-generation district heating and cooling network serving a shopping mall in Giugliano in Campania, Naples.

The study conducted by Calise *et al.* [9] considers the integration of a 2.3 MW photovoltaic (PV) field to meet part of the mall's electricity demand, which in the Reference System (RS) is entirely supplied by the grid, along with two thermal energy storage tanks incorporated into the existing DHC network.

When photovoltaic generation exceeds the mall's electrical demand, the renewable surplus, rather than being injected into the grid, can be harnessed by the system's heat pumps (HPs). Through this Power-to-Thermal strategy, heating or cooling energy is produced and stored in the phase change material tank, thereby enhancing self-consumption and improving the mall's overall energy autonomy.

System Description – Reference System (RS)

The case study focuses on a large shopping center located in Giugliano in Campania, Southern Italy, the "Grande Sud". For the purposes of the analysis, eight commercial buildings (CBs) are considered, as illustrated in Figure 15. Among them, four share identical geometric characteristics and are therefore grouped as Type A commercial buildings (CBs-A). The remaining structures differ in size and configuration and are classified as Type B (CB-B), Type C (CB-C), Type D (CB-D), and Type E (CB-E).

Figure 15. Satellite picture of the commercial buildings [9]

For the calculation of the baseline electrical demand of the users, the contribution of indoor LED lighting and various electric equipment was considered, including computers, monitors, video surveillance systems, automated checkouts, cash registers, POS terminals, and outdoor parking area lighting.

This baseline demand was then combined with the electrical consumption of the HVAC system to determine the total electric load ($E_{el,LOAD}$) for the case study.

It is worth noting that, although the shopping mall opens to the public at 9:00, the HVAC system is switched on at 8:30 to ensure that comfortable indoor conditions are reached before customers arrive. This operating schedule follows the requirements of D.P.R. 412/1993.

In the reference configuration, the entire electricity demand is supplied by the grid, which powers both the building's electrical systems and the HPs.

The thermal plant is equipped with four Aermec NRG 3200H heat pumps [10], providing a total heating capacity of 3.59 MW and a cooling capacity of 3.44 MW.

These units deliver thermal energy to two thermal rings, each with a volume of 616 m³, the main components of the investigated 4th generation district heating and cooling network. The layout of the ring system is shown in Figure 16.

Air distribution is managed by eight Air Handling Units (AHUs), each dedicated to conditioning one of the commercial buildings within the complex

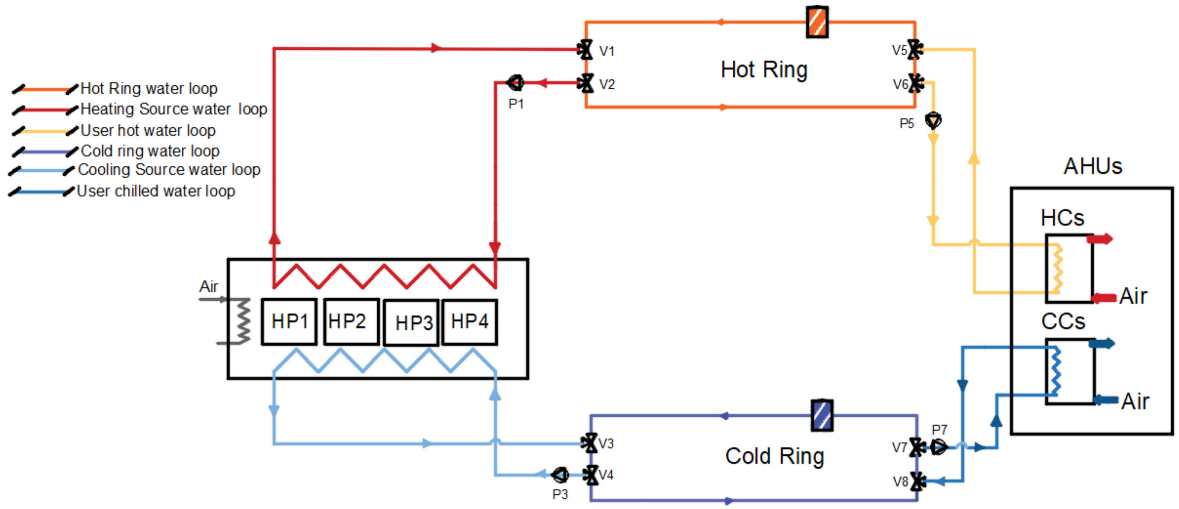

Figure 16. Reference system layout [9]

System Description – Proposed System (PS)

In system proposed by the authors, referred to as PV-P2T, a portion of the mall's electrical demand is covered by a PV field. To further optimize the use of renewable resources and limit the amount of surplus electricity injected into the grid, thereby reducing issues such as instability, and voltage fluctuations, a P2T strategy is adopted.

Through this approach, excess renewable electricity is converted into thermal energy by means of heat pumps and subsequently stored in dedicated tanks containing both water and phase change materials (PCM-TKs).

Specifically, two units are integrated into the thermal plant: H-PCM-TK, used for heating energy storage, and C-PCM-TK, designed for cooling energy storage, as illustrated in Figure 17.

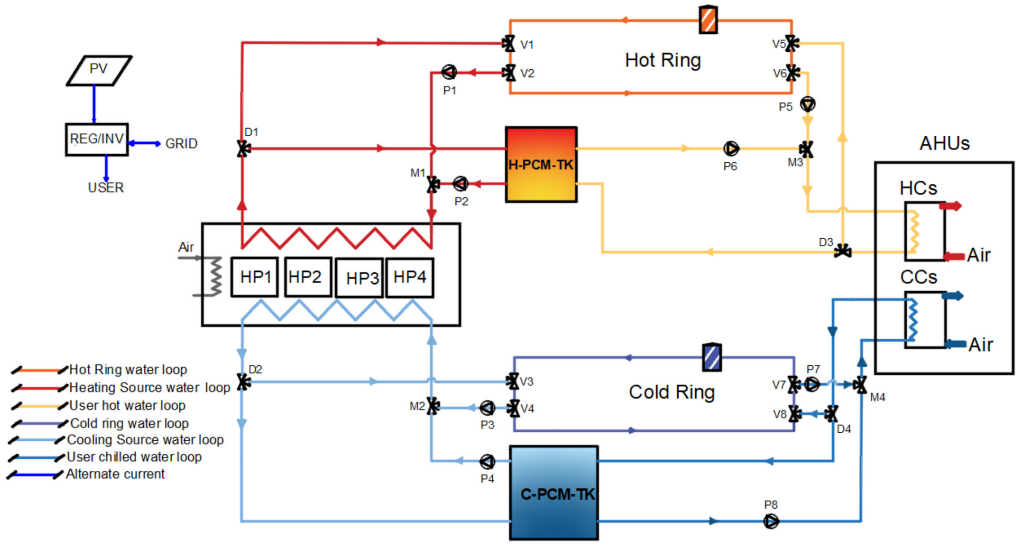

Figure 17. Proposed system layout [9]

Since SP9 GEL is employed for low-temperature storage, the analysis focuses on the charging and discharging processes of the C-PCM-TK.

Compared to the PCM adopted by the researchers, ATP 12, the operating temperatures of SP9 GEL are slightly lower; consequently, the model and the corresponding temperature settings have been adjusted accordingly.

The charging of the C-PCM-TK occurs under two conditions:

1. The surplus power generated by the photovoltaic panels ($P_{el,PVexcess}$) must be sufficient to supply at least one heat pump ($P_{el,ratedHP}$);
2. At least one heat pump must be available for charging, meaning that not all units are simultaneously engaged in balancing the thermal ring.

If these two conditions are not simultaneously fulfilled, the surplus electricity is delivered to the grid. Otherwise, the thermal charging of the PCM-TK units is governed by a staged control strategy of the heat pumps.

A temperature sensor installed in the lower section of the tank supervises the charging process: when the measured temperature drops below 12 °C, the first heat pump is activated. Each additional decrease of temperature of 1.25 °C triggers the activation of an additional heat pump. The sequence continues until the temperature reaches 7 °C, at which point the C-PCM-TK is considered fully charge.

Once the storage tank is charged, the discharge control strategy to satisfy the cooling demand must be defined.

It would be inefficient to use the energy stored in the PCM if renewable power is directly available; therefore, the first condition to enable discharging is that the PV production is lower than the demand. In addition, a second control is implemented to verify that the tank is sufficiently charged: if the sensor located in the bottom section records a temperature of 13 °C or lower, the tank is used to remove heat from the cooling coils.

DYNAMIC SIMULATION

To predict the operating conditions of the shopping mall HVAC system, a dynamic simulation was carried out in TRNSYS 18, which provides detailed models for all system components. In this framework, the behaviour of the PCM tank is modelled through Type 840, according to the model developed at the Institute of Thermal Engineering, as reported in reference [11].

To simulate the phase-change process of the PCM, the enthalpy approach [12], in which enthalpy is defined as a continuous and invertible function of temperature, is adopted. Based on

this assumption, an energy balance is applied to the different nodes of the storage system, allowing the temporal evolution of enthalpy and, consequently, of temperature to be determined. This method makes it possible to overcome the issue of the nearly constant temperature observed during the phase transition within the tank.

The tank is discretized into *N* horizontal segments. Each segment, referred to as node (j), is characterized by three parameters: enthalpy (h_j), temperature (T_j) and mass (m_j). For every node, the energy balance is formulated as follows:

$$m_j \frac{h_j^{p+1} - h_j^p}{\Delta t} = \dot{Q}_{dp}^p + \dot{Q}_{hx}^p + \dot{Q}_{aux}^p + \dot{Q}_{cond}^p + \dot{Q}_{loss}^p \quad (4)$$

The left side of the equation represents the enthalpy evolution in node (j) from the time step (p) to the time step p+*1*, where Δt denotes the time step size. The right-side accounts for the heat flows entering and leaving the node, defined as follows:

- $\dot{Q}_{dp}^p$ is the heat flow associated with the mass flow through a connection, referred to as a double port. The model allows up to five possible connections, each of which can be assigned a direction and a reference node.
- $\dot{Q}_{hx}^p$ represent heat exchange with an internal heat exchanger, which can itself be discretized into nodes adjacent to those of the tank. A maximum of five internal heat exchangers can be defined.
- $\dot{Q}_{aux}^p$ denotes heat input from a built-in auxiliary heater.
- $\dot{Q}_{cond}^p$ is the heat conduction between adjacent storage nodes.
- $\dot{Q}_{loss}^p$ indicates thermal losses to the surrounding environment.

For the correct operation of Type840, it is necessary to define correctly the material contained in the tank and its thermophysical properties.

The case analysed by the authors concerns an aluminium water tank containing cylindrical PCM modules. The tank geometry was defined in the study and subsequently used unchanged for the dynamic simulation; the corresponding values are reported in **Table 4**. The table also lists the number of PCM modules installed, together with the masses of water and PCM. Finally, the overall thermal storage capacity of the tank is provided, calculated as follows:

$$C_{ap} = m_{wat} c_{wat} \Delta T_{rated,wat} + m_{PCM} \Delta h_{rated,PCM} \quad (5)$$

The equation reports the sum of the sensible heat stored by the water and the latent heat associated with the PCM's phase change. It should be noted that this rated thermal capacity is an ideal upper bound.

Table 4. Design parameters of PCM tanks [9]

Parameter	Description	Value	Unit
V_{PCM-TK}	Total inside volume of the storage tank	532.68	m^3
$V_{PCM\ modules\ in\ TK}$	Inside volume of PCM modules in the storage tank	335.56	m^3
$V_{water\ in\ TK}$	Inside volume of water in the storage tank	197.12	m^3
H_{PCM-TK}	Height of the cylindrical storage tank	8.79	m

Parameter	Description	Value	Unit
$d_{\mathrm{PCM-TK}}$	Diameter of the cylindrical storage tank	8.79	m
λ_{eff}	Effective vertical thermal conductivity of water in the storage tank	2	W/m K
N_{modules}	Number of cylinder modules	9111	-
$d_{\mathrm{outer\ diameter}}$	Outer diameter of cylinder module	0.087	m
H_{module}	Height of cylinder module	6.15	m
m_{PCM}	Mass of PCM inside the tank	453	t
m_{water}	Mass of water inside the tank	196.12	t
C_{ap}	Rated thermal capacity	18.25	MWh
$V_{\mathrm{PCM-TK}}$	Total inside volume of the storage tank	532.68	m^3
$V_{\mathrm{PCM\ modules\ in\ TK}}$	Inside volume of PCM modules in the storage tank	335.56	m^3

The outputs of the dynamic simulation are pivotal to assess the effectiveness of the P2T strategy under varying PV production conditions and across different PCM solidification and melting cycles. In addition, the temperature distribution inside the storage tank is analysed to verify the thermal stratification, a phenomenon previously observed during the laboratory experiments.

RESULTS

The results were obtained by dynamic simulations that accounted for the operation of the photovoltaic plant proposed by the authors and the electricity demand of the shopping mall on a representative summer day, August 29th. This day was selected to evaluate the behaviour of the PCM under realistic late-summer operating conditions rather than peak extremes. This approach allows the investigation of system operations during periods when photovoltaic generation and cooling demand are both substantial, yet not extreme, thereby avoiding the optimistic bias typically associated with design-day scenarios.

Since the primary objective of this analysis is to assess the performance of the phase change material and the impact of the P2T strategy, no thermo-economic evaluation of the proposed system is carried out in this paper. Details about the results of the thermo-economic analysis were discussed in reference [9].

The simulation was carried out with a time step of 90 seconds, which allows for an accurate representation of the short-term variations in both electrical and thermal loads, as well as the charging and discharging cycle of the PCM tanks.

As shown in Figure 18, whenever excess photovoltaic production $P_{\mathrm{el,EXCESS}}$, is available and at least one HP is not engaged in supplying the cold ring, the C-PCM-TK is charged. This is highlighted by the value of $P_{\mathrm{el,P2T}}$, which marks the conversion of surplus electricity into thermal flowrate stored in the PCM tank. Such operation reduces the amount of electricity delivered to the grid.

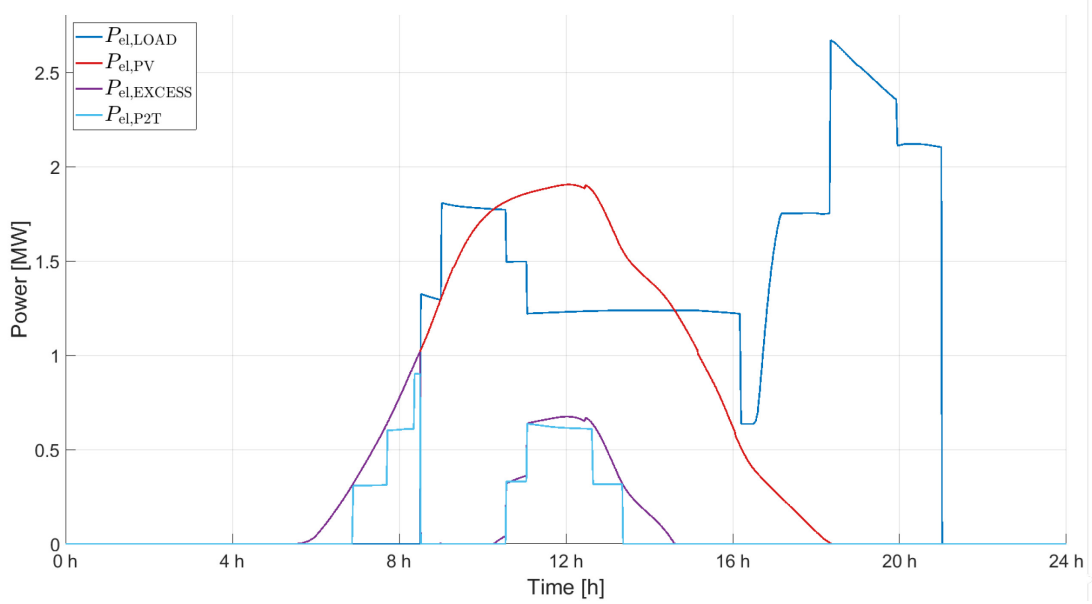

Figure 18. Dynamic results showing the effectiveness of P2T strategy

Whenever the electrical load exceeds PV power production, electricity is imported from the grid, whereas any surplus that cannot be used for the operation of the heat pump is delivered to the grid. With the integration of SP9 GEL, part of this surplus is instead stored as thermal energy: specifically, 72.39% of the available PV excess was used to charge the PCM rather than being delivered to the grid. As a result, the heat pumps supplying the cold ring can be completely switched off in the afternoon, approximately between 16:00 and 20:00, as indicated by the zero value of $P_{el,CHs}$ during this time range in **Figure 19**. This reduces the electricity demand of the shopping mall compared to the case without storage.

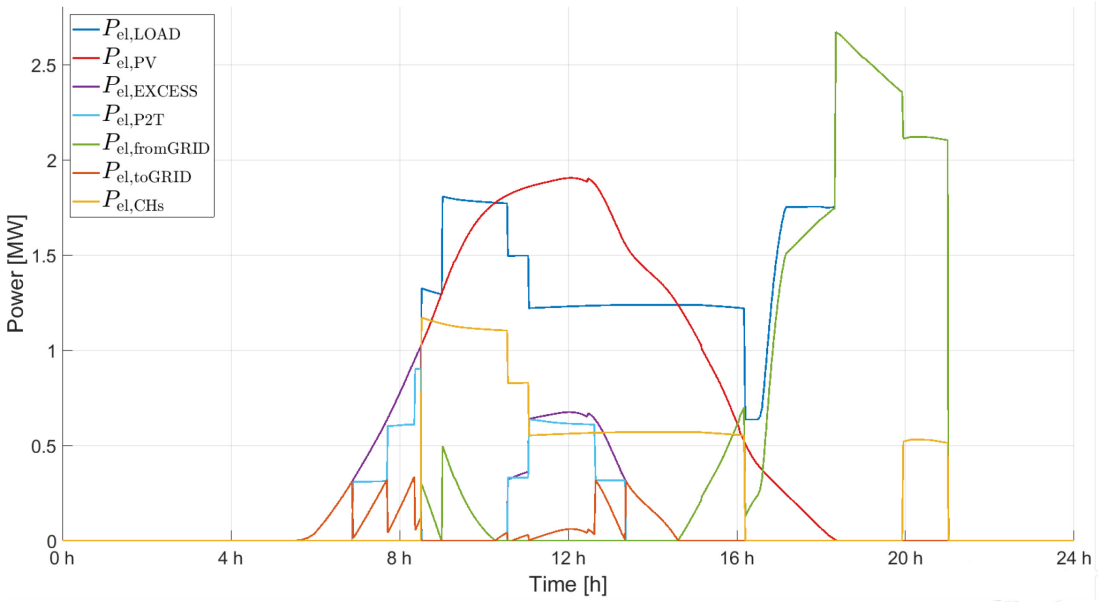

Figure 19. Power profiles during summer day

To better understand the dynamics of the tank operation, **Figure 20** illustrates the cooling process of the C-PCM-TK, whenever excess renewable electricity is available. Once the tank is charged, the PCM is then exploited to completely cover the cooling demand during the afternoon hours.

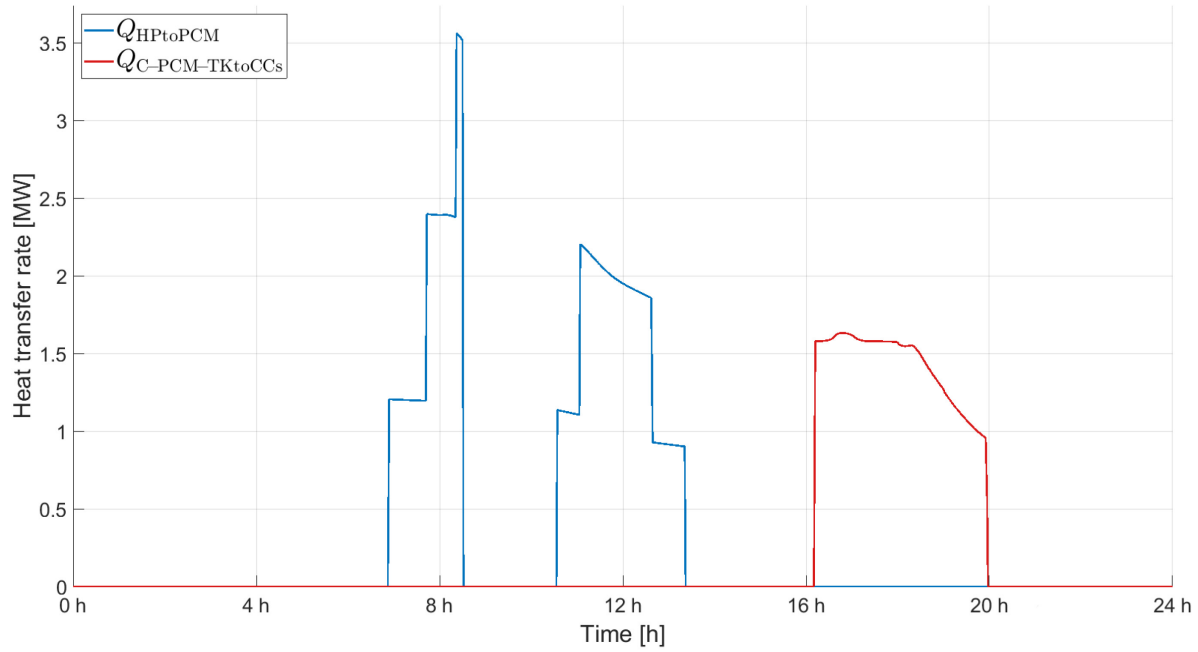

Figure 20. Charing and discharging cycle

Finally, **Figure 21** and **Figure 22** reports the temperatures obtained by five sensors positioned at different heights along the vertical axis of the C-PCM-TK. Each sensor records both the water temperature T_{wat}, the temperature at the core of the cylindrical PCM modules $T_{\text{PCM,in}}$, and the temperature at their external surface $T_{\text{PCM,ext}}$.

No PCM modules are installed at sensor levels 1 and 5; consequently, PCM temperatures are unavailable at these positions and only T_{wat} is reported.

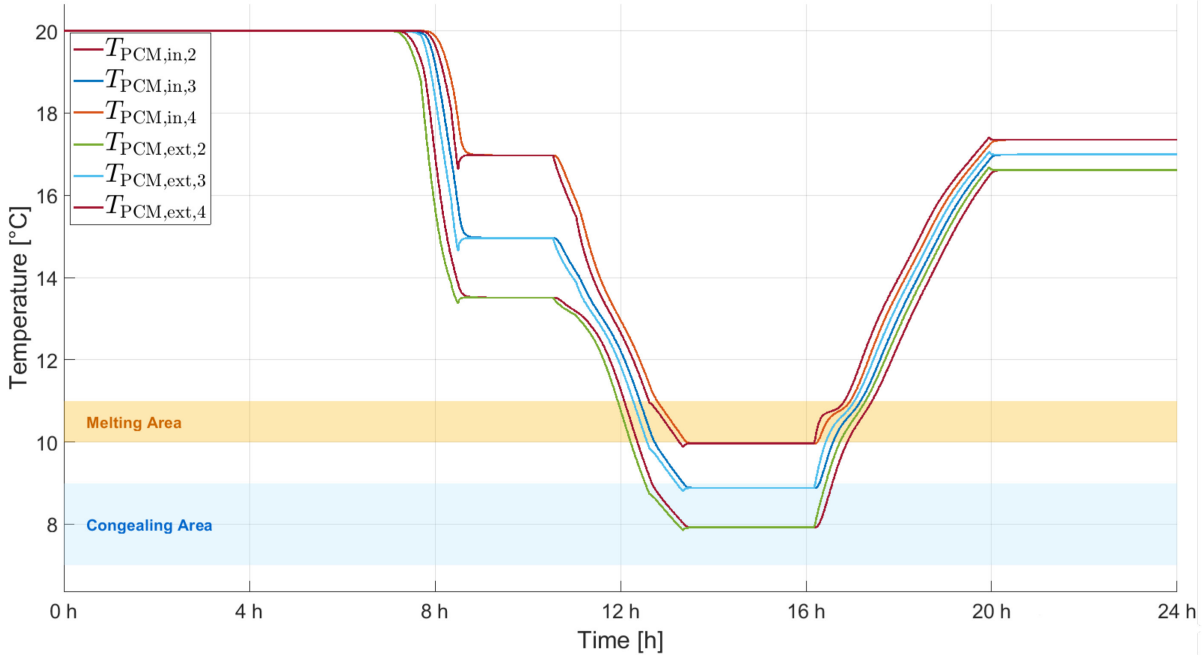

Figure 21. Temperature inside the tank over time: PCM temperature

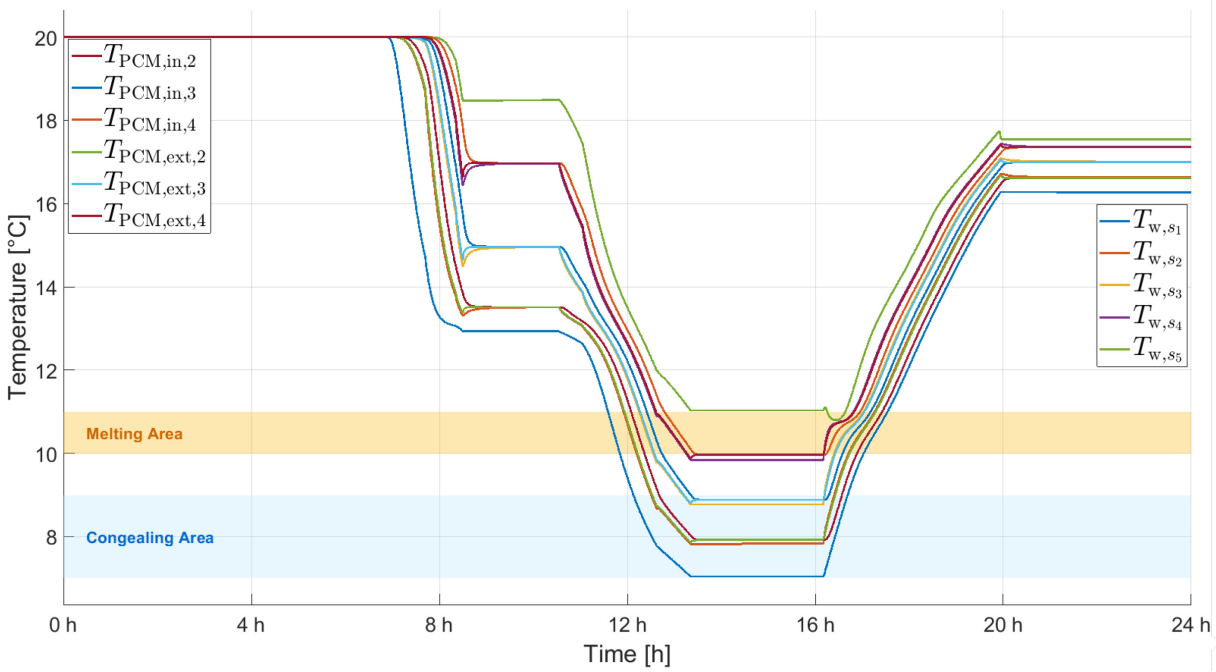

Figure 22. Temperature inside the tank over time: PCM and water temperature

During the operation, the tank continues to be used until both the water and the PCM reach 16 °C, in order to maximise utilisation and to harness the sensible heat accumulated during the charging phase.

Consistent with the laboratory tests presented in previous chapter, these profiles again reveal pronounced vertical stratification. The PCM located in the upper section of the tank does not enter the congealing area, thereby not fully utilising the tank's storage capacity.

This outcome reflects the adopted geometry, with model dimensions representative of multiple tanks arranged in series. Constructing a single 532.68 m³ vessel would be typical of industrial plants rather than a shopping centre. Since the TRNSYS Type 840 employed allows the representation of one tank only, the set of N storage units was idealised as a single equivalent vessel with the same total volume.

DISCUSSION

The study shows that thermal storage with a phase change material can valorise surplus photovoltaic electricity, providing an alternative pathway to store variable renewable output. The SP9 GEL was evaluated beyond the laboratory set up, in an operationally realistic context, to observe its behaviour under application conditions.

According to the previous analysis [9], the P2T strategy, despite being coupled with high-energy-density thermal storage, does not translate into substantial annual energy savings in shopping centres when both heating and cooling seasons are considered.

This limited impact is primarily due to winter operation. During the colder months, the availability of solar radiation significantly decreases, which in turn limits the amount of excess photovoltaic electricity that can be diverted to charge the thermal storage tanks. Consequently, the potential contribution of the P2T approach remains marginal, since most of the electrical demand must still be met directly by the grid.

The operation is markedly different during summer months, when the high solar radiation increases the amount of surplus renewable energy available for storage and the P2T strategy becomes far more effective. Previous analyses report that, in August, 44.29% of the PV energy excess can be successfully stored as thermal energy [9]. This result is confirmed by the investigated case study, where the performance of the P2T strategy reaches its peak: for a

typical summer day (August 29th), 72.39% of the photovoltaic surplus was converted into thermal energy and stored in the C-PCM-TK rather than delivered to the grid.

Beyond the site-specific quantitative results, the analysis highlights several transferable insights. The findings confirm that PCM solidification constitutes the dominant limiting mechanism for the performance of low-temperature cold thermal energy storage systems. Moreover, the simulations demonstrate the strong influence of tank geometry and heat-exchanger configuration on both charging rate and thermal stratification within the PCM. In the present case, the pronounced stratification is primarily associated with the large height of the storage tank adopted in the TRNSYS model. Since the selected TRNSYS Type represents the storage system as a single equivalent vessel, a single large tank was modelled instead of multiple smaller units. In practical applications, the deployment of several shorter tanks arranged in series or parallel could reduce stratification effects and enhance the effective utilisation of the PCM volume.

Overall, the results indicate that, while PCM-based cold thermal storage can effectively enhance photovoltaic self-consumption during favourable summer conditions, its performance is strongly governed by physical constraints related to phase change dynamics, system geometry, and seasonal solar availability. These findings are broadly applicable beyond the specific case study and provide useful guidance for the design and assessment of PCM-based P2T solutions in future renewable-integrated district energy systems.

From a broader technological perspective, electrical storage systems should not be interpreted as alternatives to the proposed approach. Their integration with PCM-based thermal storage can further increase onsite renewable self-consumption and enhance overall system flexibility.

Another possible option is ice thermal storage, which may appear attractive from a cost perspective. However, this technology presents inherent operational limitations due to the fixed phase change temperature of water at 0 °C. Consequently, ice production requires chillers to operate under sub-freezing conditions, an operating regime that many existing cooling systems are not designed to support [13].

Sensible water storage represents a simpler and generally more cost-effective solution, but it is characterised by a lower energy density and typically requires significantly larger storage volumes to achieve comparable capacity [14]. In this context, PCM-based storage can be regarded as an intermediate solution, combining higher energy density within a narrow temperature range with compatibility with conventional low-temperature cooling systems.

CONCLUSION

In this work, a combined experimental and dynamic investigation was performed to evaluate the suitability of SP9 GEL as a phase change material for space cooling within the broader context of thermal energy storages. The experimental activity, carried out over five months at the Process and Energy Laboratory of Delft University of Technology, aimed to characterise the material thermal response within the temperature operating range of 8 – 10 °C.

The experimental campaign focused on determining the duration of the charging and discharging phases and on evaluating strategies to accelerate solidification, which represents the main performance bottleneck in low-temperature PCM systems.

Three charging methods were examined:

1. Cooling the material from the bottom through a single heat exchanger;
2. Enhancing the effective heat-transfer surface by modifying the PCM geometry;
3. A dynamic configuration in which the container was periodically rotated during charging.

The results demonstrated that the dynamic rotation method substantially improved solidification. Preventing the formation of insulating layers and maintaining effective contact

between the liquid PCM and the cooled surfaces, rotation reduced the charging time by more than 70 % compared to the baseline configuration.

According to the experimental characterisation, SP9 GEL was integrated into a fourth-generation district heating and cooling network serving the "Grande Sud" shopping mall in Naples, Italy.

Dynamic simulations performed in TRNSYS 18 replaced the ATP-12 PCM adopted in earlier studies with the material tested experimentally, allowing the evaluation of the material performance under realistic operating conditions.

The analysis focused on a representative summer day characterised by high solar availability and substantial cooling demand. Despite the large height of the storage tank, which prevented full solidification and led to partial thermal stratification, the combination of water and cylindrical PCM modules enabled the heat pumps supplying the cold ring to be completely switched off for approximately four hours in the afternoon, with the cooling load satisfied entirely by the PCM tank.

On the same day, 72.39% of the photovoltaic surplus was stored as thermal energy rather than delivered to the grid, confirming the effectiveness of the Power-to-Thermal approach under favourable summer conditions. However, these encouraging results show a marked seasonal dependence. During winter, the limited solar irradiance severely reduces the renewable surplus available for charging, significantly constraining the contribution of the P2T strategy.

Furthermore, during summer months, thermal storage offsets only the electricity associated with heat-pump operation, while the demand from lighting, appliances and other services continues to be met by the electric grid. This underscores the value of integrated solutions that can address both thermal and electrical loads.

Building on these findings, several avenues for future development emerge. Improving the thermal conductivity of SP9 GEL, for example through the inclusion of nanoparticles or other high-conductivity additives, could accelerate solidification and enhance storage efficiency.

The use of modular, shorter tanks arranged in series or parallel may help limit stratification and increase the effective utilisation of the PCM volume.

Finally, coupling PCM-based thermal storage with electrical storage systems such as lithium-ion batteries offers a promising pathway to increase onsite renewable self-consumption and further reduce reliance on the grid, particularly during periods of low solar availability.

NOMENCLATURE

Symbols

$P_{\mathrm{el,LOAD}}$	electrical power demand of the shopping mall	[MW]
$P_{\mathrm{el,PV}}$	electrical power generated by the photovoltaic system	[MW]
$P_{\mathrm{el,EXCESS}}$	excess electrical power not directly consumed by the mall	[MW]
$P_{\mathrm{el,P2T}}$	electrical power converted into thermal power	[MW]
$P_{\mathrm{el,fromGRID}}$	electrical power imported from the grid	[MW]
$P_{\mathrm{el,toGRID}}$	electrical power exported to the grid	[MW]
$P_{\mathrm{el,CHs}}$	electrical power input to the heat pumps supplying the cooling ring	[MW]

Q_{HPtoPCM}	thermal power transferred from the heat pumps to the PCM tank	[MW]
$Q_{\mathrm{C-PCM-TKtoCCs}}$	thermal power delivered from the cold PCM tank to the cooling coils	[MW]
$T_{\mathrm{PCM,in,j}}$	inner temperature of the cylindrical PCM modules at sensor level j	[°C]
$T_{\mathrm{PCM,ext,j}}$	external temperature of the cylindrical PCM modules at sensor level j	[°C]
$T_{\mathrm{wat,s,j}}$	water temperature inside the storage tank at sensor level j	[°C]

Abbreviations

AHU	Air Handling Unit
CTES	Cold Thermal Energy Storage
DHC	District Heating and Cooling
HVAC	Heating, Ventilation and Air Conditioning
HP	Heat Pump
HTF	Heat Transfer Fluid
P2T	Power-To-Thermal
PV	Photovoltaic
PS	Proposed System
RS	Reference System
TES	Thermal Energy Storage
4GDHC	4TH Generation District Heating and Cooling

REFERENCES

1. International Energy Agency, Buildings, https://www.iea.org/energy-system/buildings, [Accessed: Sept. 15, 2025].
2. Jokiel, M., Development and Performance Analysis of an Object-Oriented Model for Phase Change Material Thermal Storage, (Technical) Report, SINTEF, Trondheim, Norway, 2016.
3. Alam, M., Zou, P. X. W., Sanjayan, J. and Ramakrishnan, S., Energy saving performance assessment and lessons learned from the operation of an active phase change materials system in a multi-storey building in Melbourne, Applied Energy, Vol. 238, pp 1582-1595, 2019, https://doi.org/10.1016/j.apenergy.2019.01.116.
4. Tan, P., Lindberg, P., Eichler, K., Löveryd, P., Johansson, P. and Sasic Kalagasidis, A., Thermal energy storage using phase change materials: Techno-economic evaluation of a cold storage installation in an office building, Applied Energy, Vol. 276, 115433, 2020, https://doi.org/10.1016/j.apenergy.2020.115433.
5. Chunovkina, A. and Chursin, A., Guide to the Expression of Uncertainty in Measurement, Report, Joint Committee for Guides in Metrology, Sèvres, France 2008.
6. Zipf, V., Neuhäuser, A., Willert, D., Nitz, P., Gschwander, S. and Platzer, W., High temperature latent heat storage with a screw heat exchanger: Design of prototype, Applied Energy, Vol. 109, No. 1, pp 462-469, 2013, https://doi.org/10.1016/j.apenergy.2012.11.044.

7. Zhang, Y., Liu, S., Yang, L., Yang, X., Shen, Y. and Han, X., Experimental study on the strengthen heat transfer performance of PCM by active stirring, Energies, Vol. 13, No. 9, 2238, 2020, https://doi.org/10.3390/en13092238.
8. Eslamnezhad, H. and Rahimi, A. B., Enhance heat transfer for phase-change materials in triplex tube heat exchanger with selected arrangements of fins, Applied Thermal Engineering, Vol. 113, pp 813-821, 2017, https://doi.org/10.1016/j.applthermaleng.2016.11.067.
9. Calise, F., Cappiello, F. L., Cimmino, L., Cuomo, F. P. and Vicidomini, M., A 5th generation district heating cooling network integrated with a phase change material thermal energy storage: A dynamic thermoeconomic analysis, Applied Energy, Vol. 389, 125688, 2025, https://doi.org/10.1016/j.apenergy.2025.125688.
10. Landes Energie Agentur Hessen, Large Heat Pump, https://grosswaermepumpen-info.de, [Accessed: Sept. 25, 2025].
11. Heinz, A., Moser, C., Schranzhofer, H. and Puschnig, P., Model for the transient simulation of water- or PCM slurry-tanks with integrated PCM modules, Report, Graz University of Technology, Graz, Austria, 2022.
12. Claußen, T., Entwicklung und experimentelle Verifizierung eines dynamischen Latentwärmespeichermodells (in German, Development and Experimental Verification of a Dynamic Latent Heat Storage Model), M.Sc. Thesis, University of Oldenburg, Oldenburg, Germany, 1993.
13. Dinçer, I. and Rosen, M. A., Thermal Energy Storage: Systems and Applications, John Wiley & Sons, Hoboken, New Jersey, 2021.
14. Hooman, K., Mobedi, M. and Tao, W.Q., Solid–Liquid Thermal Energy Storage: Modeling and Applications, Taylor & Francis Group, Boca Raton, Florida, 2022.

Paper submitted: 29.12.2025
Paper revised: 11.02.2026
Paper accepted: 20.02.2026